**Iranian Journal of Geophysics, Vol 20 No 3, 2026, Page 1 – 27 (Research Article)**
**DOI: 10.30499/ijg.2026.435424.1567**

# Investigation of temporal changes of seismicity and magnetic parameters before earthquakes with a magnitude of around 6 in Iran in 2017

Pooyan Hassan Beygi [1], Ali Moradi [2*] and Mohammad Javad Kalaee [3,2]

[1] *M.Sc., Institute of Geophysics, University of Tehran, Tehran, Iran*
[2] *Associate Professor, Institute of Geophysics, University of Tehran, Tehran, Iran*
[3] *Associate Professor, Department of physics education, Farhangian University, Tehran, Iran*

(Received: 12 January 2025, Accepted: 18 March 2026)

## Abstract

This study examines temporal changes in seismicity and solar-geomagnetic parameters prior to moderate-to-large earthquakes in Iran during 2017-2018, with emphasis on the evolution of the Gutenberg-Richter b-value as a potential indicator of changing seismic regime. We selected five significant earthquakes for detailed analysis. While the study primarily focuses on main shocks with magnitudes around 6, the 2017 M 5.2 Malard (Tehran) earthquake was specifically included due to its proximity to the capital, affecting a population of over 10 million, and its status as the most significant instrumental event near Tehran in recent decades. Declustered earthquake catalogs from the Iranian Seismological Center (IRSC) were used to track b-value variations, while external parameters - including Earth's magnetic field strength, solar wind proton density, geomagnetic indices including Disturbance Storm Time (Dst) and planetary K index (Kp), sunspot number, and 10.7 cm solar radio flux (F10.7 index) concerning fluctuations in b-value preceding major earthquakes - were analyzed at daily, hourly and 27-day resolutions. In four out of five cases, the b-value showed a pronounced decrease within several weeks before the mainshock, indicating a temporary shift toward the dominance of larger-magnitude events, consistent with stress concentration patterns observed in prior studies. Four mainshocks also occurred when sunspot numbers and the F10.7 index were near their minimum values over the study period, whereas 27-day averaged proton density tended to be relatively high close to the occurrence times. Moreover, the Kp index displayed low 27-day averages for four events, and Dst and Kp indices showed localized anomalies within ±48 hours of some mainshocks. These patterns suggest possible temporal associations between seismic and solar-geomagnetic variability at monthly timescales, although no formal statistical tests were applied. However, the small number of events, uncertainties in the seismic and magnetic datasets and the absence of formal statistical testing limit the strength of any conclusions and preclude causal inference. The correlations identified here should therefore be regarded as preliminary and do not imply that solar or geomagnetic activity directly triggers earthquakes; rather, they suggest that solar-magnetic parameters may offer complementary contextual information on the evolving state of the crust when used alongside conventional seismotectonic indicators, motivating further studies with larger datasets and more rigorous statistical and physical modeling frameworks.

**Keywords:** Earthquake precursor, seismic b-value, magnetic storms, solar proton, solar activity

*Corresponding author: asmoradi@ut.ac.ir

## 1 Introduction

Iran is situated in the Alpine-Himalayan seismic belt, where the Arabian and Eurasian tectonic plates collide. This tectonic setting makes Iran one of the most earthquake-prone countries in the world. As a result, scientific research and risk mitigation efforts are essential to minimize damage and casualties caused by earthquakes. In general, studying earthquake events is vital for safeguarding lives, reducing infrastructure damage, advancing scientific knowledge, and fostering global collaboration in mitigating seismic risks.

Also, research on earthquake events contributes to developing early warning systems (Marzocchi et al., 2014; Cauzzi et al., 2016). These systems can provide alerts seconds to minutes before the shaking begins, allowing people to take protective actions and reducing casualties and damage.

On the other hand, while precise short-term earthquake prediction remains challenging, scientists often look for anomalies or changes in the Earth's behavior that might be associated with increased seismic risk (Jackson and Kagan,1999). Some potential anomalies include (1) Foreshocks; (2) Ground Deformation: Unusual ground deformation, measured using techniques like Global Positioning System (GPS) or satellite imagery, may indicate stress accumulation along faults; (3) Changes in Seismicity Patterns (Kossobokov and Shebalin, 2003); (4) Changes in Gas Emissions: Variations in radon or other gas emissions from the Earth's crust; and (5) Electromagnetic Anomalies: Unusual electromagnetic signals, such as changes in ionospheric or ground-based measurements, have been studied as potential earthquake precursors. The relationship between solar activity and earthquakes remains an open scientific question with limited consensus. While some studies have explored temporal correlations between solar events - such as solar flares and variations in solar radiation - and earthquake occurrence, these observations do not yet constitute an established physical mechanism. For example, the Simpson (1967) report contained one of the earliest mentions of the connection between solar activity - as indicated by sunspots, radio noise, and geomagnetic indices - and seismic occurrences on Earth. This study attempted to investigate if the effects of solar activity can be considered as a potential triggering mechanism for earthquakes. It used not only sunspots but also the 2800 MHz solar radio flux and the geomagnetic Kp index as indicators of solar activity. Galper et al. (1995) presented the results of measuring variations in the flux of high-energy particles during magnetically quiet periods. They showed that the observed increase in the intensity of charged particles is related to seismic activity on Earth and a temporal and spatial correlation is found between earthquakes and fluctuations in particle intensity. Their analysis of experimental data revealed a correlation between strong earthquakes and intense particle fluxes. The totality of experimental facts about the ionospheric, seismic, magnetospheric, and probably solar nature made it possible to develop a method that could potentially contribute to earthquake forecasting models or early warning frameworks.

Allan and Mason (1962) analyzed experimental data on bursts of charged particles obtained from various experiments conducted in Earth's vicinity (on the MIR space station, METEOR-3, GAMMA, and SAMPEX satellites).

Their analysis demonstrated that a considerable portion of the observed particle flux bursts correlate with seismic activity on Earth. Moreover, particle bursts have been detected several hours before major earthquakes. The L-shell locations of the particle bursts closely match the locations of the associated quakes. Certain aspects of a proposed model linking the magnetosphere and seismic events were explored in the study as well. Specifically, the model considers the interaction between electromagnetic radiation emanating from seismic events with radiation belt particles.

In their 2016 study, Cataldi et al. (2016) examined a potential link between the M7.0 earthquake that occurred near Kumamoto, Kyushu, Japan on April 15, 2016, at 16:25:06 UTC and solar activity. They have previously demonstrated scientifically that a relationship exists between global seismic events with a magnitude 5 or greater and solar activity. Additionally, they have explained instances when major earthquakes, which can also generate tsunamis, consistently coincide with changes in the density of interplanetary ions. In their 2016 work, they specifically investigated whether such a relationship connected the Kumamoto earthquake and the conditions of the Sun.

Novikov et al. (2020) stated that studies carried out so far on the relationship between earthquakes and solar processes have yielded ambiguous and contradictory results. They argue that the chief shortcoming of these studies is that they do not offer a physical account of how abrupt shifts in space weather could generate earthquakes. Grounding their view in findings from field and lab experiments showing that pulsed DC inputs into the Earth's crust can spur quakes, they propose that analogous triggering effects might arise from intense electromagnetic radiation associated with solar flares or geomagnetic storms impacting fault zones primed for seismic activity. However, more research is still needed to flesh out and examine mechanistic models clarifying the precise physical pathways through which space weather fluctuations appear coupled to seismicity.

While there have been studies indicating statistical correlations between solar activity and certain types of earthquakes, it's crucial to approach this topic with caution. The scientific community generally remains skeptical about the direct influence of solar activity on triggering large earthquakes. The processes governing earthquakes are primarily associated with tectonic activity, such as the movement of tectonic plates and the release of accumulated stress along faults.

This study examines seismic activity in Iran between 2017 and 2018, focusing on the b-value and its changes as an earthquake precursor, since monitoring such variations over time can provide insights into regional seismicity. Additionally, we investigate electromagnetic parameters before these earthquakes to determine potential associations between alterations in electromagnetic components and seismic parameters. Specifically, we explore whether variations in solar and electromagnetic parameters can serve as precursors to major earthquakes

We consider several parameters such as the Earth's magnetic field strength, solar wind proton density, geomagnetic indices like Disturbance Storm Time (Dst) and planetary K index (Kp), sunspot number, and 10.7 cm solar radio flux have been examined concerning fluctuations in b-value preceding major earthquakes. The Dst index is a measure of the intensity of the ring current flowing

westward around Earth in the magnetosphere. A negative Dst value indicates a magnetic storm, where the magnetic field generated by the intensified ring current opposes Earth's dipole field (Loewe and Prölss, 1997). The Kp index provides a 3-hour resolution of global geomagnetic activity, quantifying disturbances in the horizontal component of Earth's magnetic field caused by solar particle radiation. These indices are critical for monitoring space weather conditions that may theoretically interact with the Earth's crust through electromagnetic coupling mechanisms (Menvielle and Berthelier, 1991). The underlying concept is that external stresses from space weather and solar activity may influence stresses and pressures in Earth's crust, leading to changes in seismicity and fault instability that could be reflected in b-value alterations.

It should be clearly stated that this study does not aim to integrate seismic and magnetic datasets quantitatively, as such integration would entail extensive modeling of potential interactions, which exceeds our current scope and resources. Instead, we analyze changes in each dataset independently and present them side-by-side for visual comparison. This approach allows readers to discern which parameters - seismic (e.g., b-value) or magnetic (e.g., proton density, Dst) - exhibit the most notable variations before the events. While prior research has investigated mutual effects between these data types (e.g., Cataldi et al., 2016; Marchitelli et al., 2020), our focus remains on documenting individual temporal changes to evaluate if literature-claimed patterns are observable in these Iranian earthquakes, without confirming or refuting interdependencies.

## 2 Data

Since our aim was to investigate the existence of a correlation between magnetic and seismic data, two datasets were considered:

1) Data related to seismic events in 2017-2018 using data from the Iranian Seismological Center (IRSC).
2) Data related to magnetic field and changes in proton density (using satellite and ground data).

### 2.1 Seismic Data

The selection of the five main earthquakes in this study was based on the statistical assessment of Iran's 2017 seismicity reported by Moradi et al. (2018). That year recorded over 18,000 earthquakes, showing a 60% increase in total activity compared to the previous decade. However, among these, five events with magnitudes ≥ 5 were identified as the most significant in terms of energy release, regional impact, and data completeness. While 23 events with M≥5 occurred during this period, these five specific events were selected because they were the largest in their respective clusters and occurred in regions with sufficient seismic network coverage to allow for reliable b-value calculation. Smaller events or those in border regions with high azimuthal gaps in station coverage were excluded to minimize location and magnitude uncertainties. These events were thus selected as representative cases for detailed analysis:

- the Sefidsang earthquake in Razavi Khorasan and North Khorasan (M5.7);
- the Sarpol Zahab earthquake in Kermanshah (M7.3);
- the Hojedk earthquakes (three events with magnitudes ~6.0-6.1 in a short period) in Kerman province;
- the Sumar earthquakes in Kermanshah province (M6.0); and

- the M5.2 Malard earthquake in Tehran province.

It should be noted that although the M5.2 Malard earthquake in Tehran province was out of our considered magnitude range, it was included due to its significant importance: it is the closest and largest instrumentally recorded earthquake of M>5 to central Tehran in the past century, directly affecting a population of approximately 10 million in this megacity.

As emphasized by Moradi et al. (2018), although improvements in the national seismic network contributed to a higher number of recorded small events, the rise in medium and large earthquakes in 2017 reflects a genuine increase in seismic activity rather than a purely observational artifact.

Uncertainty estimates obtained from ZMAP indicate that typical one-sigma errors in b-value for the analyzed catalogs range between ±0.05 and ±0.10, depending on event density and completeness threshold. The observed 20-30% decreases in b-value prior to four mainshocks therefore exceed these typical uncertainties, suggesting that the variations cannot be fully explained by catalog noise or magnitude/location errors alone, although residual uncertainty remains.

The details of the events of interest are given in Table 1. Also, the epicenter distribution of the recorded earthquakes in the country and neighboring areas in 2017-2018 is shown in Figure 1. The examined regions and related events are described below.

**Table 1.** Characteristics of seismic events investigated in this study.

| No. | Event | Mag. | Lat. & Lng. | Time (UTC) | Date |
|---|---|---|---|---|---|
| 1 | Sefidsang Khorasan Razavi | M=6.0 | 35.85°N 60.34°E | 6:09 | 04/05/2017 |
| 2 | Ezgeleh-Sarpol Zahab, Kermanshah | M=7.3 | 34.77°N 45.76°E | 18:18 | 12/11/2017 |
| 3 | Hojedk Kerman | M=6.2 | 30.72°N 57.33°E | 2:32 | 01/12/2017 |
| 4 | Mallard of Tehran province | M=5.2 | 35.67°N 50.95°E | 19:57 | 20/12/2017 |
| 5 | Sumar, Kermanshah province | M=5.6 | 33.71°N 45.96°E | 6:59 | 11/01/2018 |

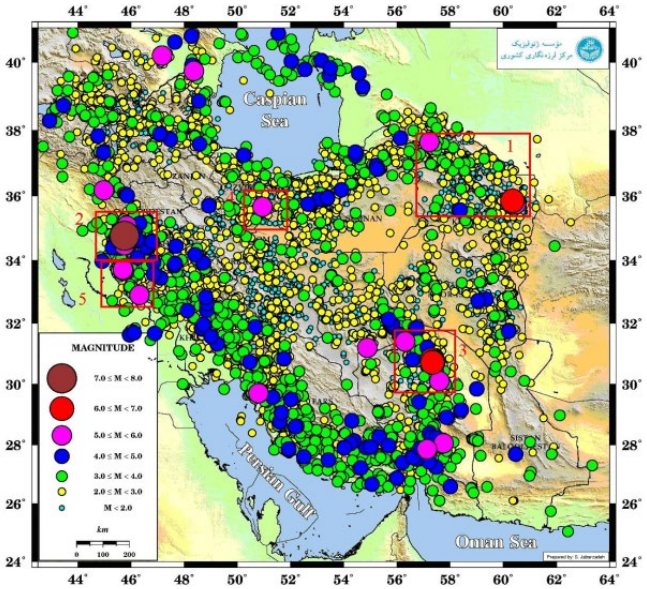


**Figure 1.** Distribution of epicenters of earthquakes recorded in Iran and nearby areas in 2017-2018 (Moradi et al., 2018).

Potential artifacts related to changes in seismic network performance were considered; however, the IRSC seismic network did not undergo major configuration changes during the analyzed period, and previous assessments indicate that the increased number of recorded earthquakes in 2017 reflects a genuine rise in seismic activity rather than improved detection capability alone (Moradi et al., 2018). While it is noted in Naserieh et al. (2019) that the IRSC catalog exhibits systematic errors - such as magnitude instability of up to 0.3 units regionally, contamination by non-tectonic events (e.g., 19% quarry blasts), and depth overestimation for blasts (>10 km) - the reliability of our b-value analysis depends heavily on the completeness magnitude ($M_c$) of the seismic catalog. To ensure our data's integrity, we examined the spatial distribution of $M_c$ for the IRSC catalog based on the comprehensive study by Naserieh et al. (2019). As illustrated in Fig. 2, the $M_c$ value for the Iranian plateau during the study period (late 2016 to 2017) was approximately 2.8, confirming that the seismic network was sufficiently sensitive to detect and record all relevant events used in our sliding window analysis. So, after removing small earthquake, the observed changes in b-value are physical and not related to catalog incompleteness.

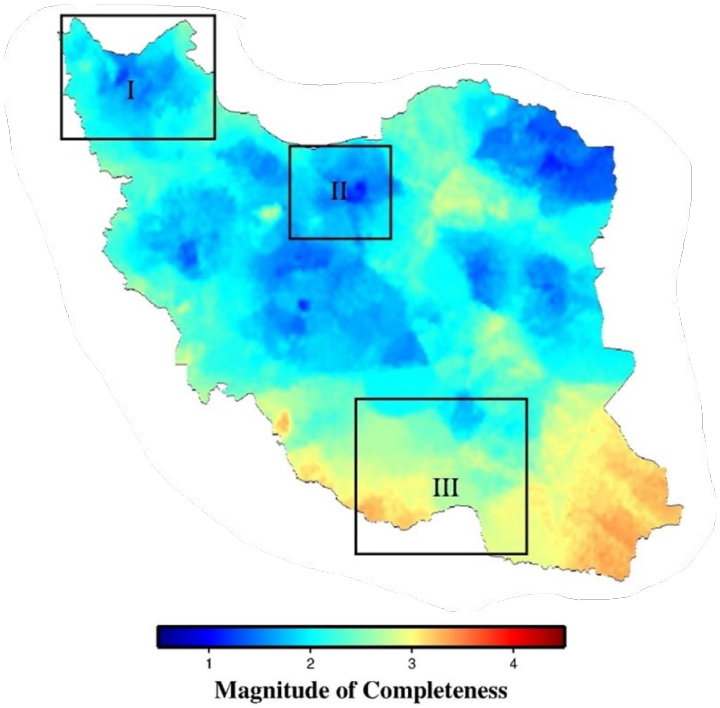


Figure 2. Spatial distribution of the magnitude of completeness ($M_c$) for the Iranian Seismological Center (IRSC) catalog across Iran. The map indicates that during the 2017 study period, the $M_c$ was consistently around 2.8 in the regions of interest, providing a robust baseline for the frequency-magnitude distribution analysis (Modified after Naserieh et al., 2019).

Seismic catalogs must be declustered to remove dependent events, such as foreshocks and aftershocks, ensuring statistical independence for frequency–magnitude analyses like b-value estimation. In this study, the Reasenberg (1985) algorithm was employed, which links events within dynamically defined

space–time interaction zones based on Omori's law and stress redistribution models, offering a more flexible approach than fixed-window methods.

Comparative studies, such as Poudyal et al. (2025) in the Kathmandu Valley - a tectonically active region akin to parts of Iran - evaluated declustering methods including Gardner-Knopoff, Gruenthal, Reasenberg, and Uhrhammer using ZMAP on 3190 events from 2000–2023. Their statistical assessments (e.g., Allan factor for temporal clustering and Morisita index for spatial distribution) showed that Reasenberg retains higher residual temporal clustering but provides a physically grounded model incorporating stress redistribution, unlike Gardner-Knopoff, which yields more homogeneous spatial distributions but may overestimate independent events. Given Iran's complex seismotectonics, Reasenberg was selected for its dynamic handling of aftershock sequences, though parameter sensitivity was mitigated by conservative choices aligned with regional decay behaviors (Reasenberg, 1985; Teng and Baker, 2019).

After loading each catalog, Figs. 3 to 5 were obtained, which show the epicentral and three-dimensional distribution of events in the 5 studied areas. The upper figures show the epicentral distribution and the lower figures show the three-dimensional distribution of these events. The left figures show the seismic events present in each catalog before declustering and the right-side figures show the same catalog after declustering. Yellow stars represent events with a magnitude greater than 5.

After declustering, the b-value changes over time were examined in ZMap software for all 5 events. For this purpose, at first, the catalogs were subjected to time series analysis in ZMap software.

The b-value is a parameter in the Gutenberg-Richter law that quantifies the relationship between the frequency and magnitude of earthquakes. A high b-value indicates a greater proportion of small earthquakes, whereas a low b-value suggests that larger earthquakes are more dominant. Thus, it is a key component in any seismic hazard assessment. Evaluating spatial variations in the b-value is one of the key components of any seismic hazard map.

Apart from its prominent importance for hazard assessment, the b-value is a valuable parameter for interpreting the mechanics of deformation and failure of rock masses. Several studies in seismology and the mining environment have supported this idea (Wesseloo, 2014).

The b-value defines the slope of the power-law relationship used to characterize the frequency distribution of earthquake magnitudes. Specifically, high b-values indicate smaller quakes prevail, while low b-values reflect large earthquakes dominating over smaller events. Variations in b-value over space and time typically serve as precursors to major seismic occurrences. Additionally, normal and thrust fault environments exhibit relatively higher and lower b-values, with strike-slip faults showing intermediate values. This suggests an inverse association between b-value and differential stress. Supporting this, studies confirm that b-values decrease as differential stress rises within continental crust. An inverse linear relationship between b-value and differential stress has also been identified along subduction boundaries. If well-constrained regionally, the link between b-value and stress could prove vitally important for tracking spatiotemporal crustal stress changes. However, reliably quantifying

this relationship depends heavily on comparable stress measurements to compute b-values (Wu, 2018).

Although b-values are approximately equal to 1 over long timescales and large spatial scales, significant variations occur at smaller scales. The b-value in earthquake swarms is often much larger than 1, sometimes reaching 2.5.

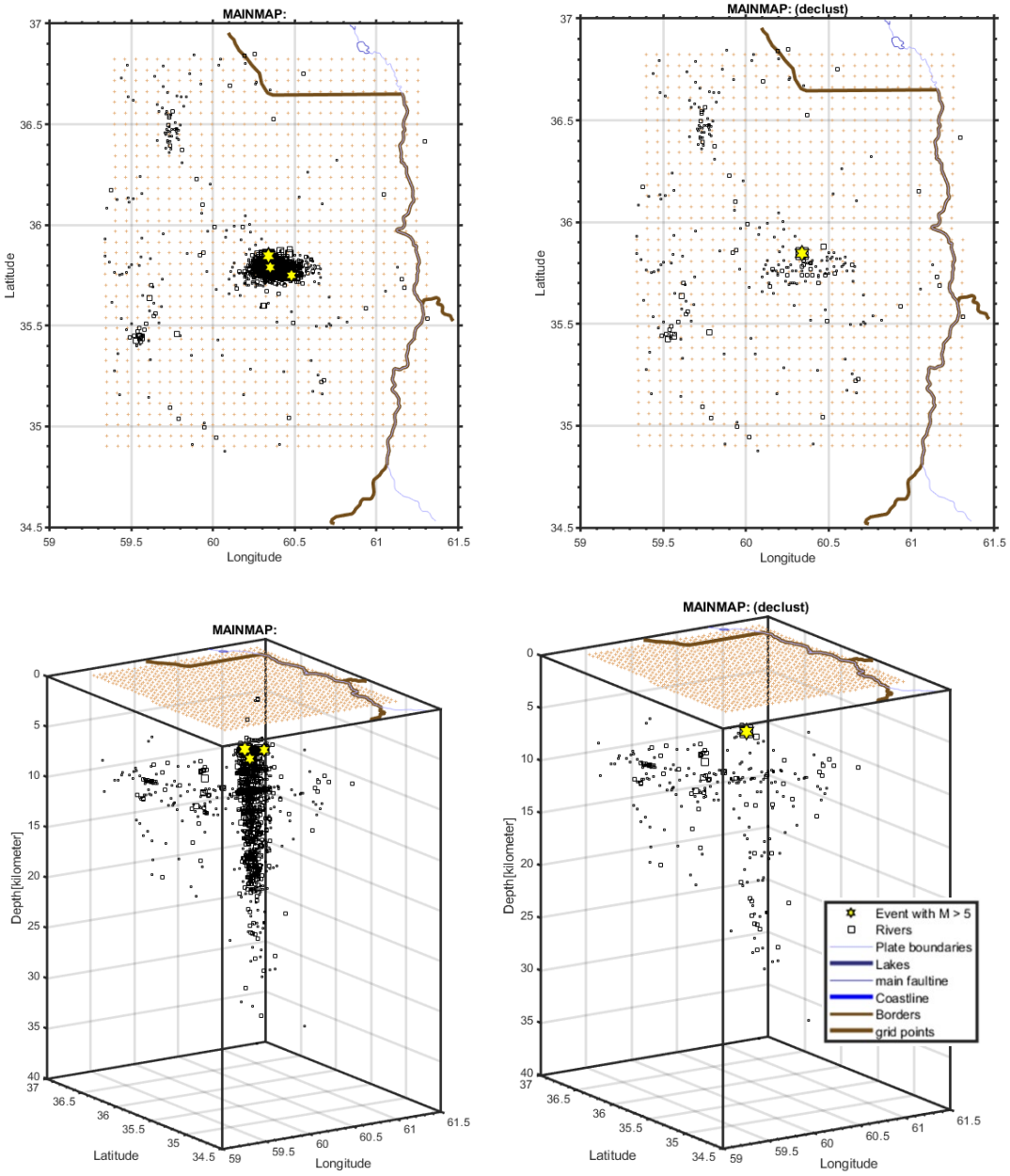


**Figure 3.** Seismic catalog processing related to seismic events recorded around the Sefid Sang area from 04/05/2016 (1 year before the main event) to 04/06/2017 (1 month after the main event). The upper figures show the epicentral distribution and the lower figures show the three-dimensional distribution of these events. Figures on the left are before declustering and figures on the right are after. Yellow stars represent events with a magnitude greater than 5. During this declustering, 11 clusters were found and 1424 events were removed from the total of 1685 events.

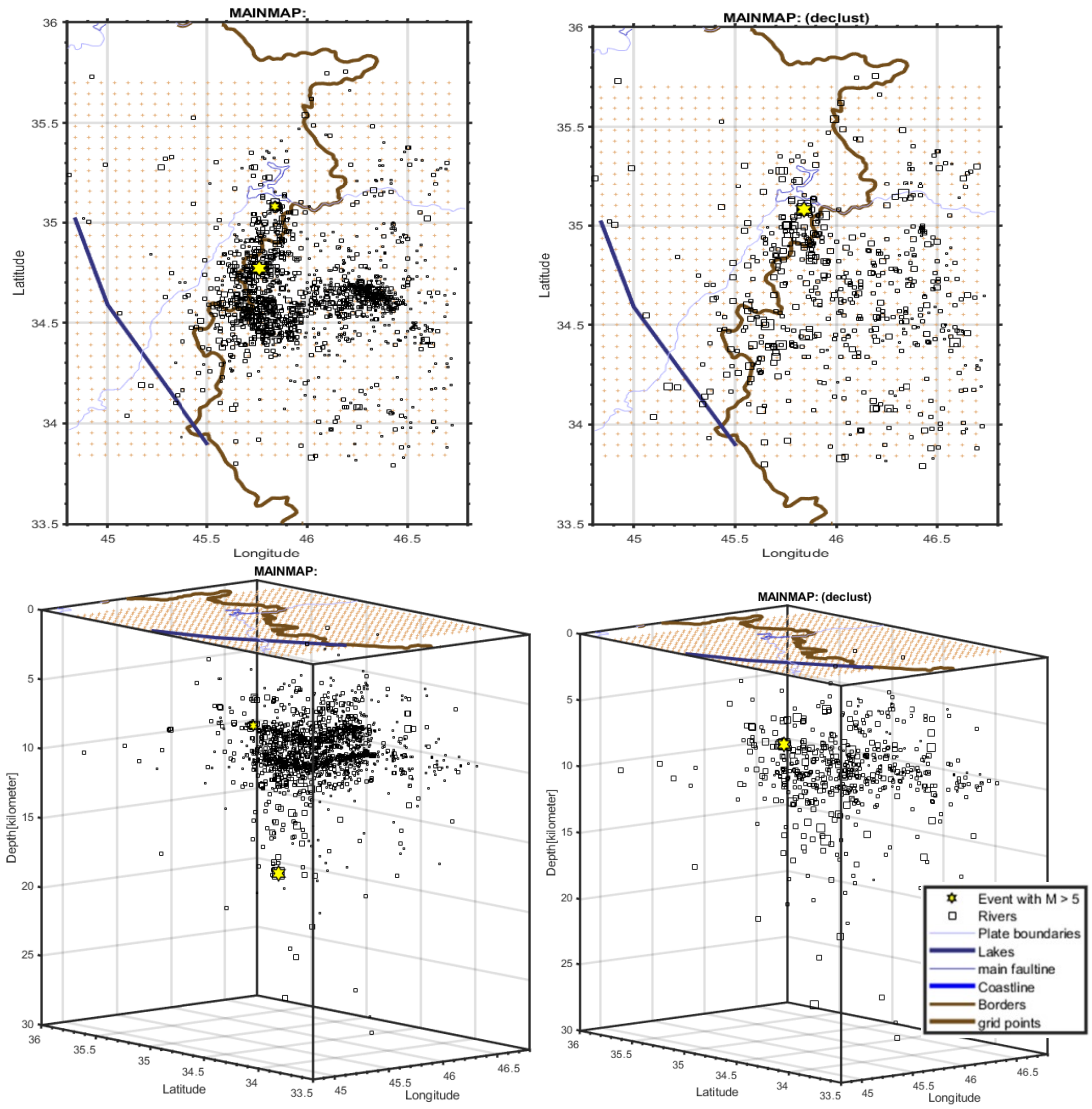


**Figure 4.** Seismic catalog processing related to seismic events recorded around Ezgeleh-Sarpol Zahab, Kermanshah area from 12/11/2016 (1 year before the main event) to 12/12/2017 (1 month after the main event). Yellow stars represent events with a magnitude greater than 5. During this declustering, 36 clusters were found and 1004 events were removed from the total of 1495 events.

One salient feature of this relationship is that it applies even to individual seismic regions, with b generally around 1. Therefore, even though the absolute number of earthquakes depends on the level of regional seismicity, the frequency distribution pattern itself remains informative. For example, it is estimated that Japan has had about 190 earthquakes with M>7 and 20 earthquakes with M>8 in the past 1300 years. Similarly, southern California has had about 180 earthquakes with M>6, 24 with M>7, and 1 with M>8 since 1816; while the New Madrid zone (central U.S.) has experienced approximately 16 tremors with M>5 and 2 with M>6 over a comparable period. Although the precise number of events depends on the period selected and uncertainty in estimating magnitude before the invention of seismographs (around 1890), the logarithmic decrease still appears (Stein, 2013).

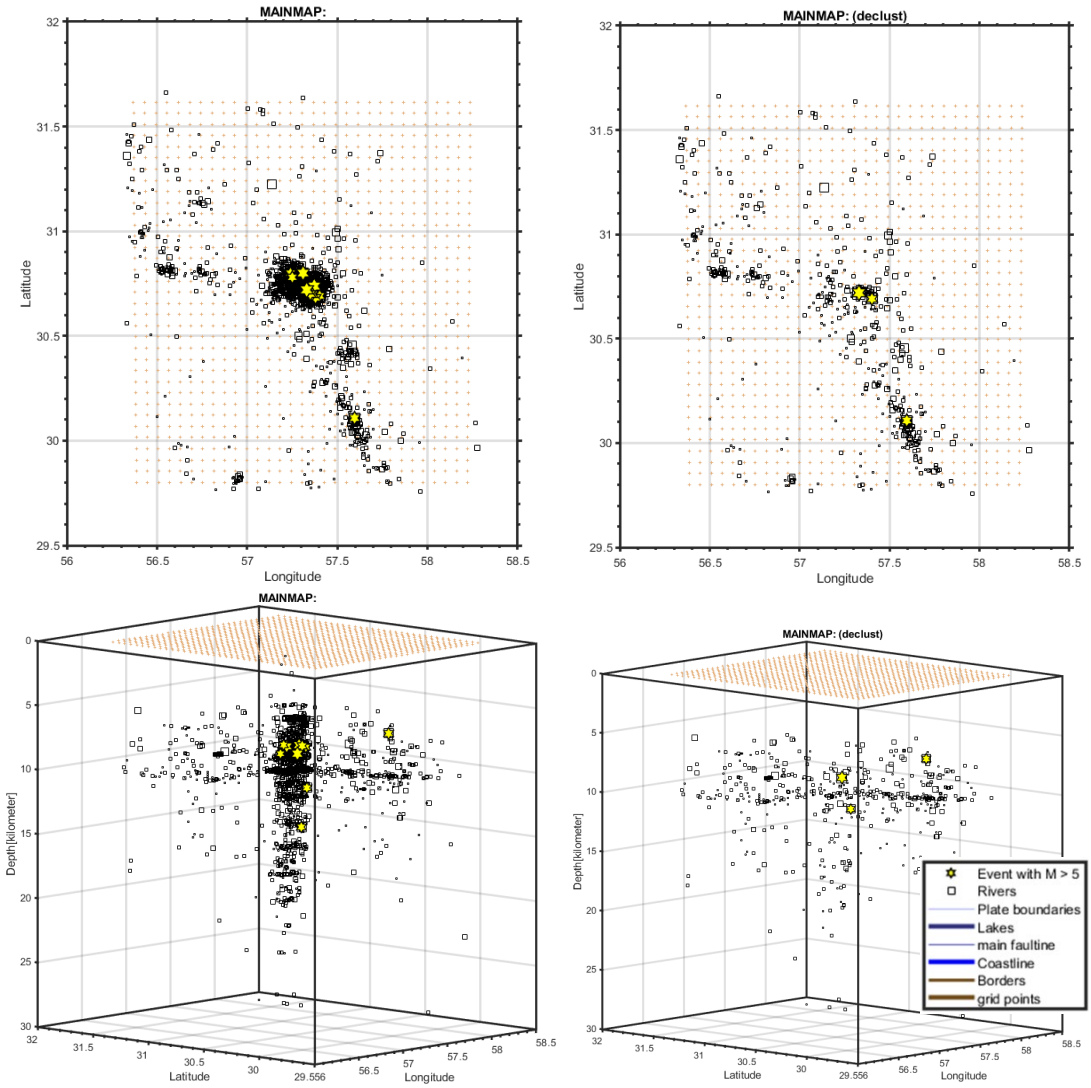


**Figure 5.** Seismic catalog processing related to seismic events recorded around the Hojedk Kerman area from 01/12/2016 (1 year before the main event) to 01/01/2018 (1 month after the main event). Yellow stars indicate events greater than 5. During this declustering, 18 clusters were found and 1622 events were removed from the total of 2099 events.

Estimating the b-value is very important for assessing earthquake probability. It has generally been assumed that b takes on values very close to 1, although depending on the catalog, estimation method, and magnitude range, variations (up to 30%) around this value have been observed (Godano, 2014). Many authors have investigated spatial or temporal variations in b (Senatorski, 2019). Numerous mechanisms have been put forward to explain the spatial and temporal fluctuations in b-value, including fracture dimensions and material attributes, stress state, pore fluid pressure, and source dynamics (Amitrano, 2003). However, some researchers argue that b-values for tectonic earthquakes do not substantially deviate from the global mean. This perspective stems from observations that the distribution of seismic moment - whose logarithm correlates with magnitude - demonstrates

remarkable stability over space and time. Therefore, according to this viewpoint, observed b-value variations may not be statistically significant given the consistency in seismic moment release (Godano, 2014).

At now, the b-value changes over time were requested and a sample window size of 100 events was considered. The default value for this number is 500, meaning that for plotting the b-value chart, it puts every 500 events in one sample window (Fig 6).

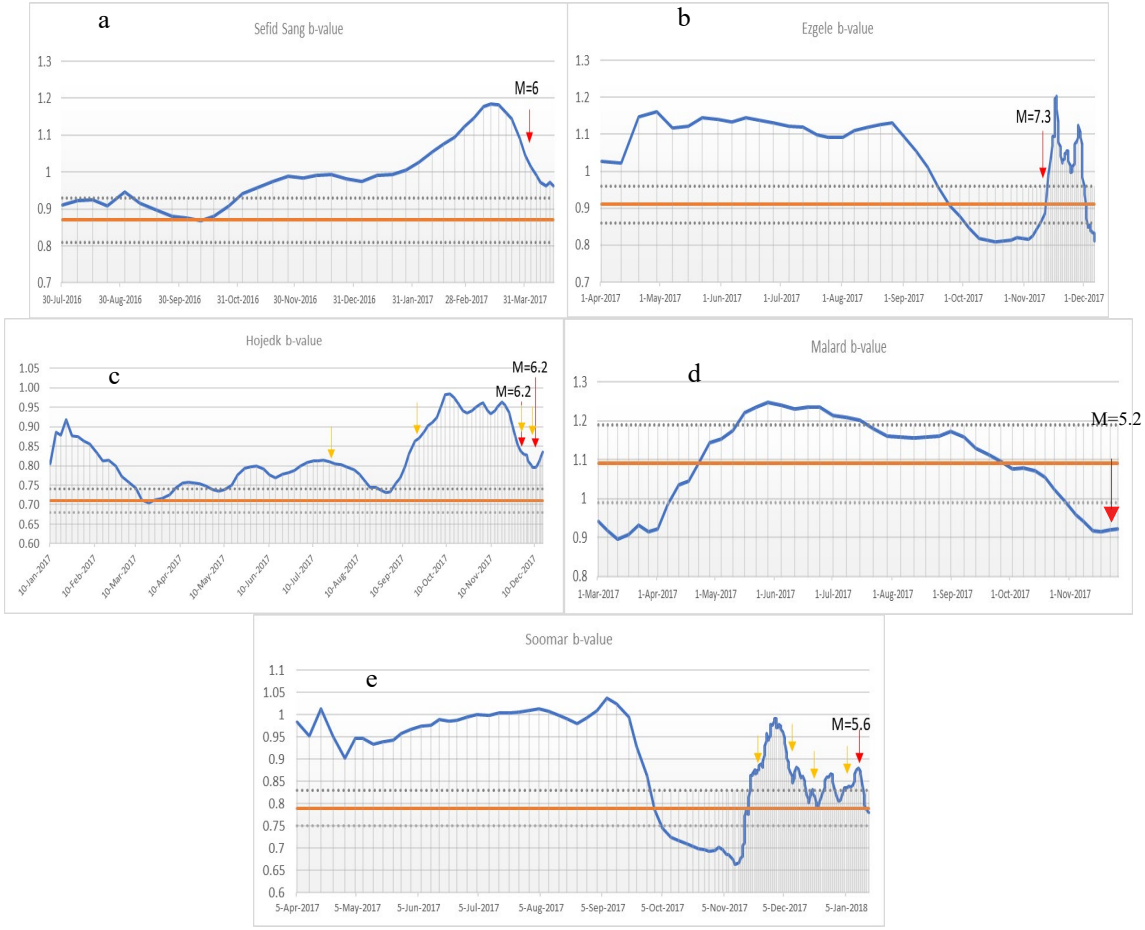


**Figure 6.** Changes of b-value with respect to time for the seismic catalogs of (a) Sefid Sang, (b) Ezgele, (c) Hojedk, (d) Malard, (e) Soomar. The orange line is the b-value using all events and the gray dots are its error. Red arrows indicate the largest event and the yellow ones indicate events larger than 5.

We evaluated b-value variations within individual regions using a consistent catalog and analysis framework. Systematic network effects are expected to affect all time windows similarly, rather than produce localized decreases prior to specific mainshocks. Within this framework, the observed b-value decreases prior to four mainshocks are more plausibly interpreted as reflecting changes in the local stress regime and evolving fault conditions, rather than artifacts of catalog incompleteness or network variability.

## 2.2 Electromagnetic Data

The magnetic data used in this study consist of changes related to parameters

such as:

- Number of sunspots
- Earth's magnetic field
- Proton density in the atmosphere
- Dst index
- Kp index
- Solar flares
- Solar F10.7 index (noise generated by the Sun at a wavelength of 10.7 cm in Earth's orbit)
- Proton flux with energies greater than 10 MeV, greater than 30 MeV, and greater than 60 MeV

Table 2 summarizes the solar and geomagnetic parameters considered in this work, including their data sources, temporal resolutions, and analysis period. This overview clarifies which parameters were examined at daily, hourly, and 27-day time scales and highlights the specific catalogs (OMNI/NOAA and SpaceWeatherLive) from which the datasets were obtained, ensuring transparency and reproducibility of the magnetic data processing."

**Table 2.** Summary of solar and geomagnetic parameters used in this study, including data source, temporal resolution and analysis period.

| ***Parameter*** | **Data Source** | **Time Resolution(s) Analyzed** | **Time Period** |
|---|---|---|---|
| *Sunspot number* | OMNI/NOAA | 1-day, 27-day | 2016/04/05-2018/04/05 |
| *F10.7 solar radio flux* | OMNI/NOAA | 1-day, 27-day | 2016/04/05-2018/04/05 |
| *Proton density (solar wind)* | OMNI/NASA | 1-hour, 1-day, 27-day | 2016/04/05-2018/04/05 |
| *Dst index* | OMNI/NOAA | 1-hour, 1-day, 27-day | 2016/04/05-2018/04/05 |
| *Kp index* | OMNI/NOAA | 1-hour, 27-day | 2016/04/05-2018/04/05 |
| *Solar flares (classification)* | SpaceWeatherLive | Event-based | 2016/04/05-2018/04/05 |

All the mentioned magnetic data (except flares and solar activity) were obtained from the database https://omniweb.gsfc.nasa.gov. This website provides the data with different time resolutions such as 5-minute intervals, 1-hour, 1-day, and 27-day (Sun's rotation period). This data is related to the period from 2016/04/05 to 2018/04/05. This time period spans approximately one year before the first studied mainshock (Sefidsang, 2017-05-04) to nearly three months after the last studied mainshock (Sumar, 2018-01-11). Figs. 7 and 8 show the solar and electromagnetic parameters in this time period with a 27-day resolution.

Regarding solar flares and activity, it is important to remember that solar flares are basically big explosions on the Sun's surface caused by twisted magnetic field lines bursting and flaring from sunspots. The definition of a solar flare is an abrupt, strong, and fast shift in brightness. When the magnetic energy built up in the solar atmosphere is suddenly released, a solar flare occurs. The data on flares and solar activity were obtained from the website https://www.spaceweatherlive.com. This website does not provide data as files and only offers charts with a maximum 24-hour range.

Solar flares are typically categorized as A, B, C, M, or X classes based on the peak 1 to 8 Angstrom X-ray flux (in Watts per square meter, $W/m^2$) measured near Earth by the XRS instrument on the GOES-15 satellite in geosynchronous

orbit. Each class is further divided into a scale from 1 to 9 on a logarithmic scale (e.g. B1 to B9, C1 to C9, etc.). An X2 flare has twice the intensity of an X1 flare, while an X4 flare is 4 times more powerful than an M5 flare. The X class scale extends beyond X9 for exceptionally intense flares sometimes termed "exceptional X class flares." For example, X10+ ranked solar flares represent extreme energetic events more powerful again than those at the X9 level.

For parameters such as magnetic field, atmospheric proton density, Kp index, and Dst index, which also fluctuate a lot at hourly resolutions, 1-hour resolution data was also obtained from the Omni web database. These parameters will be examined for 48 hours before and after each main event. Since some of these parameters have high fluctuations, their 6-hour moving average was also calculated to obtain a clearer picture of the variations. However, for the sunspot number and F10.7 solar flux parameters, only the daily resolution charts were used as they do not undergo much change on an hourly basis. A similar method was used in the paper by Urata et al. (2018) for the Kp index and in the paper by Nikouravan (2012) for the magnetic field and F10.7 index. For example, the charts related to this analysis method are presented in Figure 9.

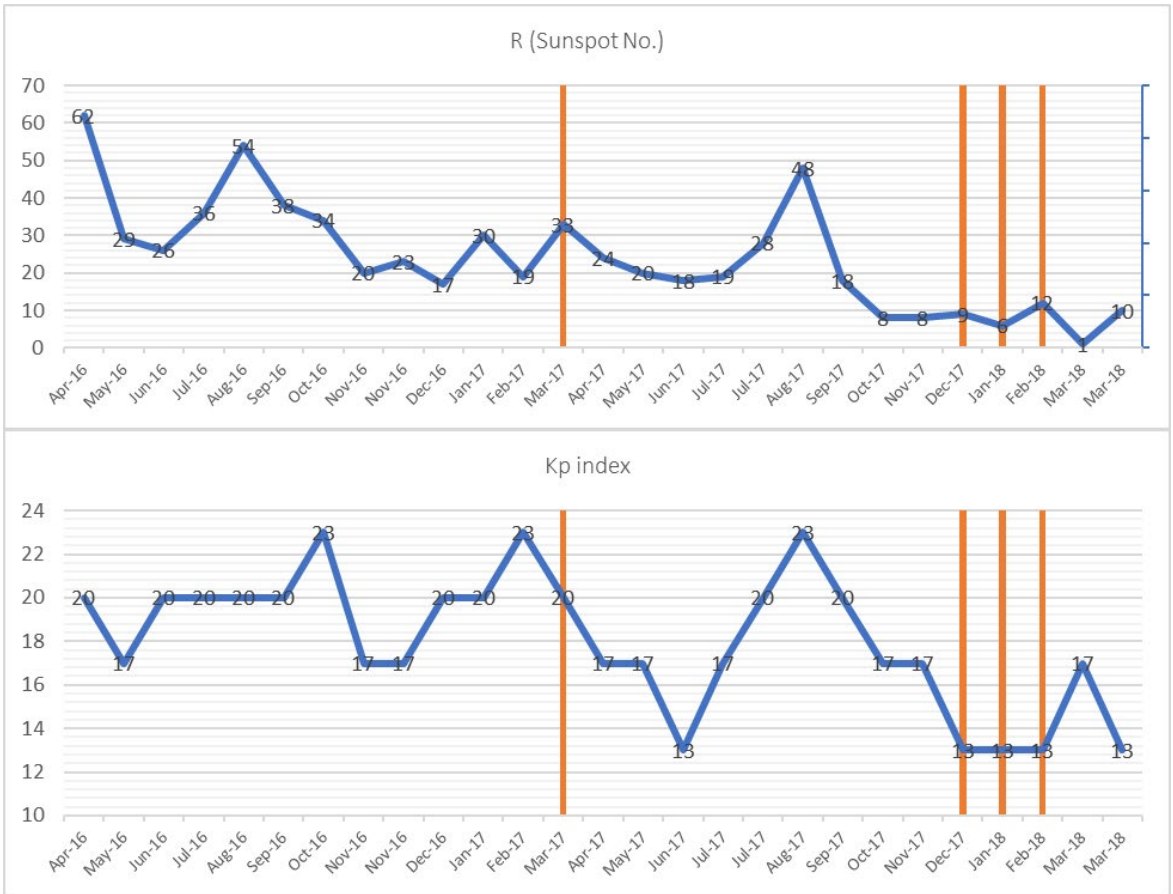

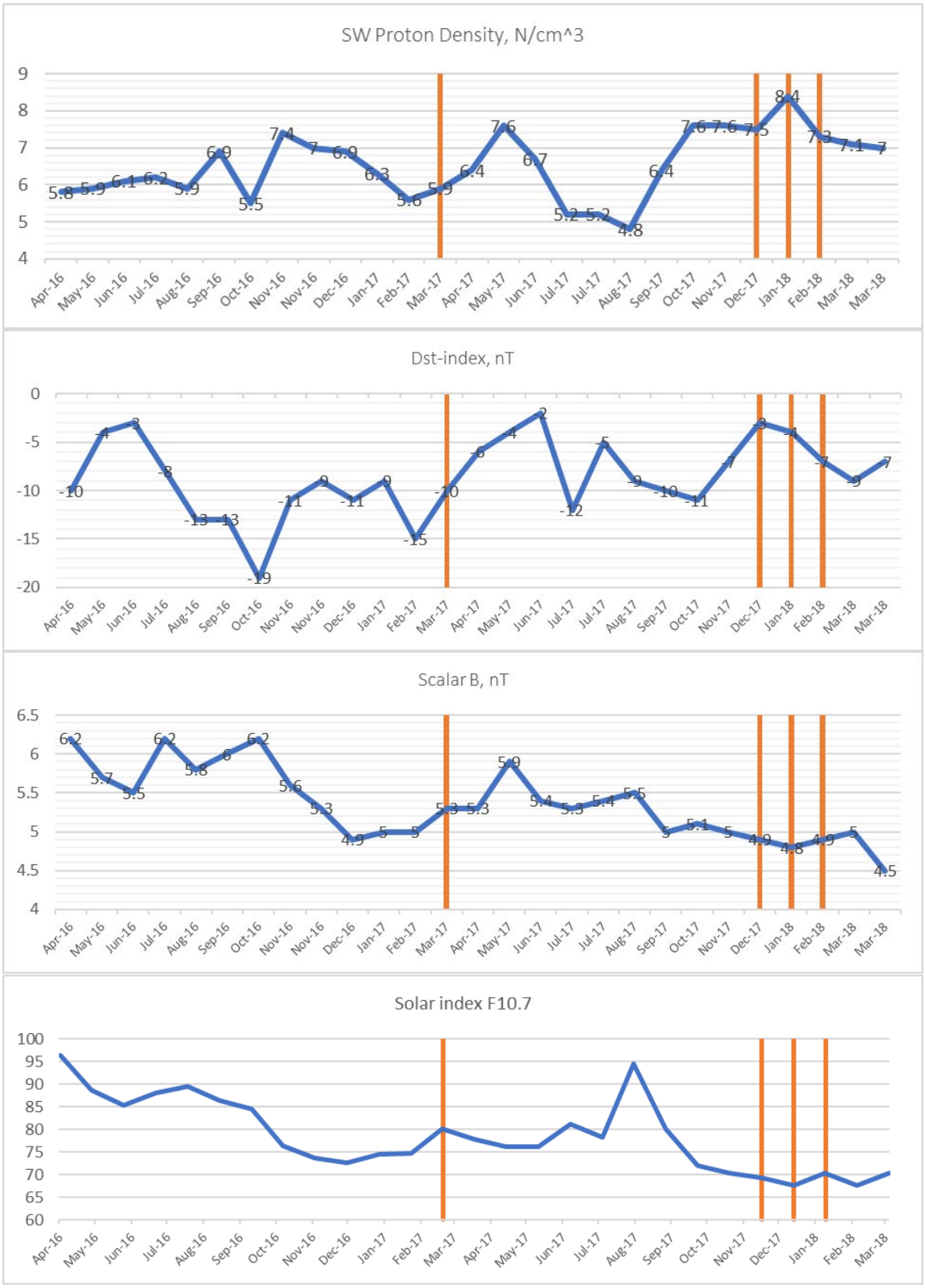


**Figure 7.** Changes in solar and electromagnetic variables from 2016/04/05 to 2018/04/05 with a 27-day resolution. Orange lines include seismic events.

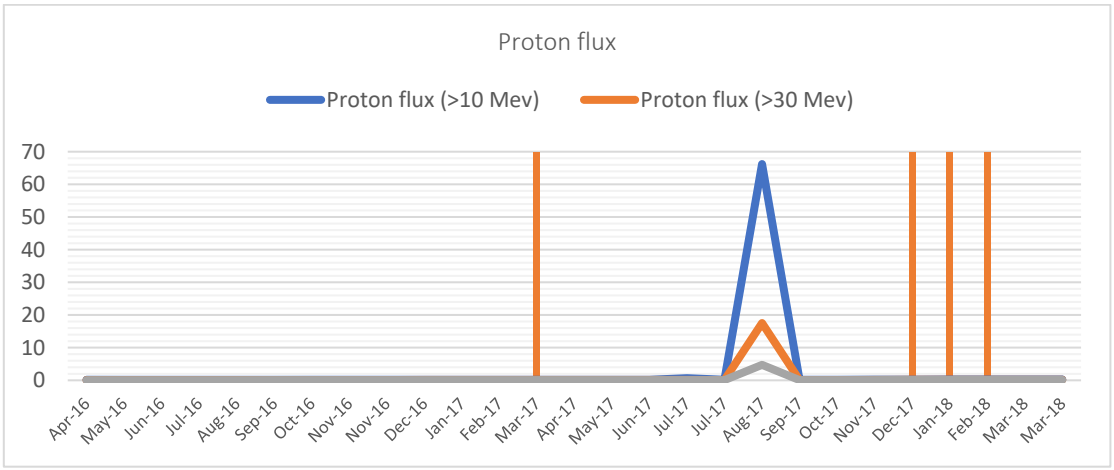


**Figure 8.** Proton flux changes with more energy than 10 Mev (blue), more than 30 Mev (Orange), and more than 60 Mev (Gray) from 2016/04/05 to 2018/04/05 with a resolution of 27 days. Orange lines include seismic events.

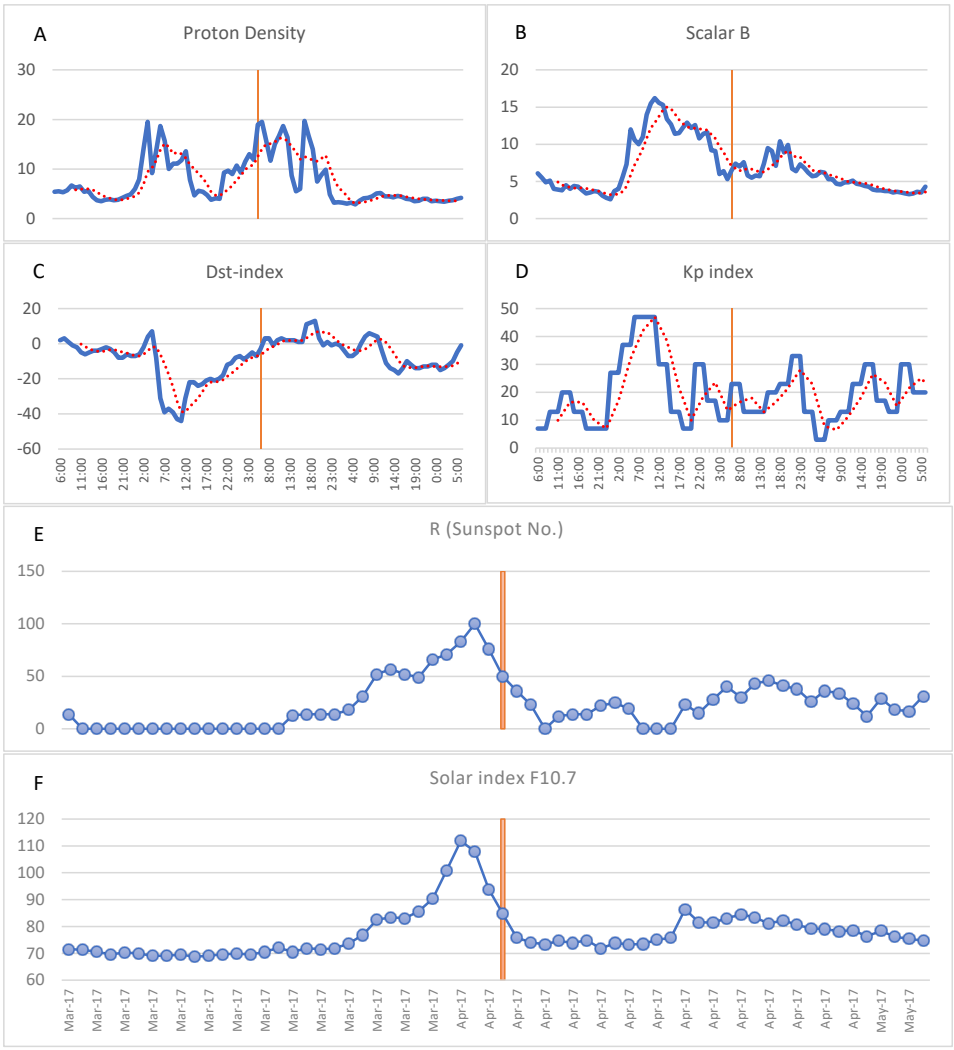


**Figure 9.** Magnetic parameter charts related to the Sefid Sang event. Charts A, B, C, and D are related to 48 hours after and 48 hours before the event and the red dashed lines show the 6-hour moving average. Charts E and F are related to 30 days after and before the event. The orange vertical lines indicate the hour and day of the main event.

The two datasets - seismic (b-value variations and mainshock timing) and magnetic/solar (sunspot number, F10.7 index, proton density, Dst, Kp indices) - were analyzed in parallel to investigate whether temporal correlations exist between magnetic parameter fluctuations and seismic activity. The underlying premise derives from previous studies suggesting that solar wind density and geomagnetic disturbances may modulate crustal stress distribution (Cataldi et al., 2016; Marchitelli et al., 2020). Specifically, we examined whether: (1) b-value changes precede mainshocks, (2) mainshocks cluster near epochs of low solar activity (low sunspot numbers and low F10.7 index), and (3) geomagnetic indices (Dst, Kp) exhibit anomalies concurrent with mainshocks. Temporal alignment was assessed through visual inspection of time series and qualitative pattern matching rather than quantitative statistical testing; thus, the results represent preliminary associations requiring further validation.

## 3 Discussion

Before discussing potential mechanisms and comparative context, we summarize the quantitative observations from this study:

(1) b-value changes: In four out of five earthquakes (80%), temporal decreases in b-value were observed 15-30 days preceding the mainshock, consistent with stress accumulation theory (Wu et al., 2018).

(2) Solar activity: Four out of five mainshocks (80%) occurred during low-sunspot epochs or days when F10.7 index values ranked in the lowest decile of the study period (Figure 7).

(3) Proton density: Four out of five mainshocks (80%) occurred near 27-day peaks in solar wind proton density, despite lower-resolution data showing no consistent pattern.

(4) Geomagnetic indices: Dst and Kp indices showed anomalous behavior (minima or rapid transitions) within ±48 hours of three mainshocks, most pronounced for the M7.3 Ezgeleh-Sarpol Zahab event.

These observations suggest potential temporal clustering rather than purely random coincidence, within the limitations of a small sample size; however, the small sample size (n=5) and absence of independent validation against a comparison dataset (e.g., random synthetic catalogs) limit quantitative inference. Each finding is discussed in the context of existing literature below."

These observations suggest potential temporal clustering, but they remain exploratory and have not been validated by formal statistical tests; therefore, they should not be interpreted as evidence of non-random behavior.

### 3.1 Mechanism of Effect

Solar-geomagnetic activity can influence the near-Earth environment through variations in solar wind conditions, coronal mass ejections (CMEs), and associated geomagnetic disturbances, which modulate the magnetosphere and ionosphere. These processes alter electric currents and electromagnetic fields that may, in principle, interact with the lithosphere.

Solar minimum conditions are typically characterized by reduced solar wind velocity and fewer intense CMEs, leading to an expansion and relative relaxation of the magnetosphere. Some studies suggest that such large-scale changes may modify boundary conditions or stress transmission pathways

within the Earth system, potentially influencing faults that are already close to failure.

One proposed mechanism involves the inverse piezoelectric effect in quartz-bearing rocks. According to this hypothesis, variations in proton density and associated electromagnetic disturbances may enhance electric potential differences between the ionosphere and the crust, driving electric currents along conductive fault zones. These currents could generate small strain perturbations through inverse piezoelectric responses, potentially modifying local Coulomb stress and slightly advancing or delaying rupture on critically stressed faults (e.g., Marchitelli et al., 2020).

However, these mechanisms remain largely hypothetical and are not quantitatively constrained for the Iranian seismotectonic setting. The present study does not attempt to model or validate such processes. Instead, solar-geomagnetic parameters are treated as contextual variables, and interpretations are restricted to observed temporal associations rather than causal relationships.

### 3.2 Relation between b-value and magnetic parameters

For the five mainshocks analyzed in this study, b-value time series exhibit pronounced decreases approximately 15-30 days prior to four events, whereas one event shows no clear precursory variation. In several cases, these decreases coincide with periods of relatively low solar activity, reflected by reduced sunspot numbers and F10.7 index values, as well as elevated 27-day averaged proton density.

Reliable estimation of b-values is inherently challenging, as results depend on factors such as catalog quality, event sampling, and the chosen statistical approach. Previous studies have demonstrated that limited sample sizes or catalog heterogeneity can distort frequency-magnitude distributions and potentially mimic apparent b-value variations.

For instance, Saltiel et al. (2011) reported deviations from a single Gutenberg-Richter relation in geothermal environments and emphasized the importance of carefully assessing catalog characteristics before interpreting b-value changes. Similarly, Shi and Bolt (1982) showed that sample windows of roughly 100 earthquakes are generally required to obtain stable b-value estimates, providing a practical guideline widely adopted in subsequent studies.

Recent studies provide important context for the observed b-value changes and solar-geomagnetic associations in the present work. Venegas-Aravena and Cordaro (2023) analytically demonstrated, using multiscale thermodynamics, a negative correlation between the Gutenberg-Richter b-value and electromagnetic signals generated during pre-macroscopic rock failure - even under constant macroscopic stress - attributing this to small-scale cracking dynamics that dominate entropy production and irreversible energy release prior to macroscopic rupture. Complementarily, Calandra and Teti (2024) analyzed 200 Italian earthquakes ($M \geq 4.3$, 1600-2022) and found statistically significant correlations between earthquake triggering/magnitude and the positions and resultant gravitational forces of the Sun, Moon, and seven Solar System planets, concluding that the “7-Planet System” exerts a stronger causal influence than traditional lunar-solar tides alone, calculated via vector physics and angular distances.

In this work, declustered catalogs and a sliding window of 100 events were used to balance temporal resolution and statistical stability. Within this framework, the observed 20-30% b-value decreases prior to four mainshocks exceed typical short-term fluctuations seen within the same catalogs, suggesting that these changes likely reflect variations in the seismic regime rather than noise alone. Nevertheless, given the limited number of events and the absence of formal statistical testing, these results should be regarded as exploratory.

### 3.3 Magnetic parameters without taking b-value into account

The magnetic parameters studied in this study are affected by solar activity. Solar activity is characterized by cycles with a period of approximately 11 years. Therefore, to discuss the magnetic parameters, we must first see where the studied seismic events fall within the solar cycle. As mentioned, Nikouravan (2012) concluded that the number of major

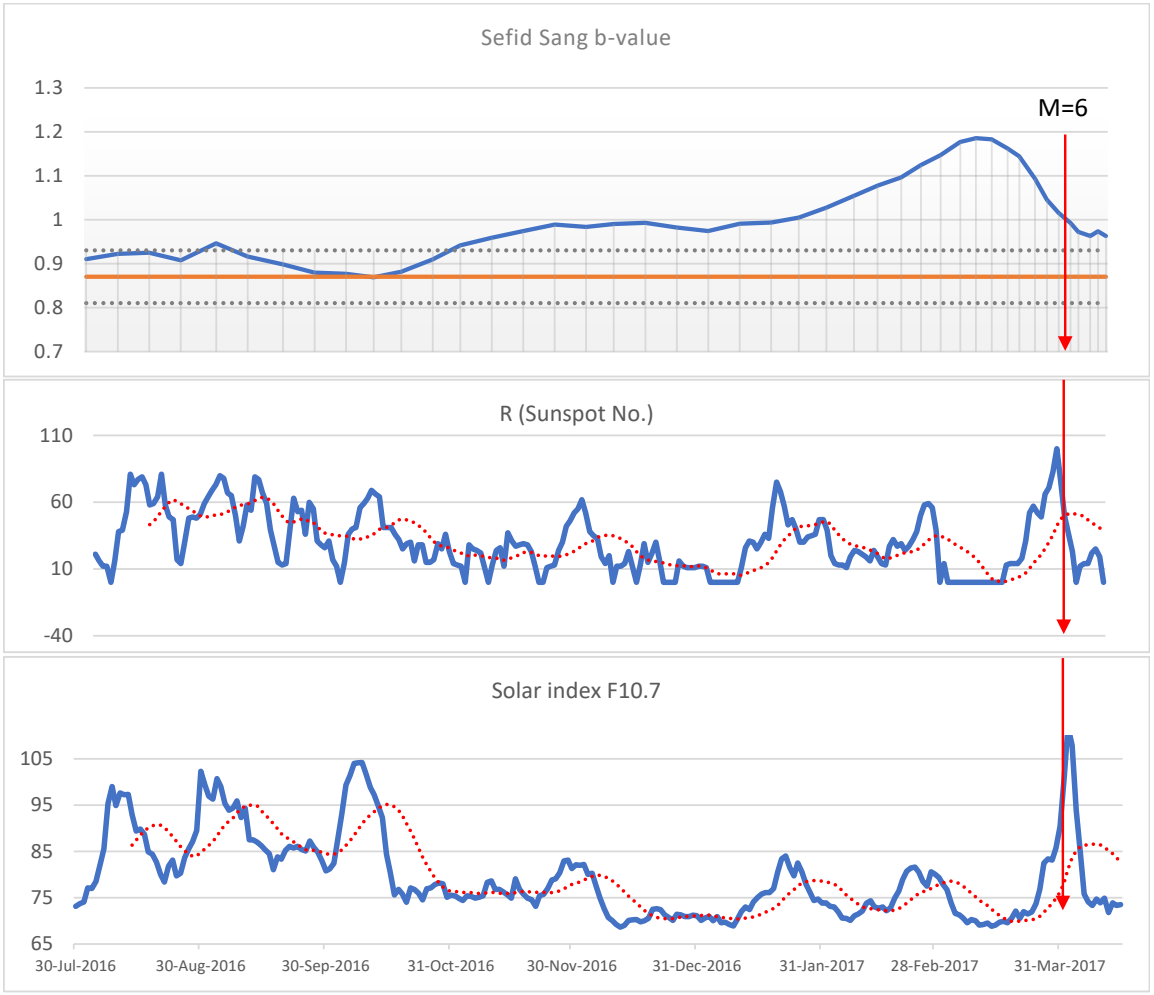


Figure 10. The variations of the b-value over time for the Sefid Sang region events (top), the variations of the sunspot number parameter (middle), and the F10.7 solar radio flux parameter (bottom) with 1-day resolution. The red dashed lines show the 15-day moving average. The red arrow indicates the day of the largest event.

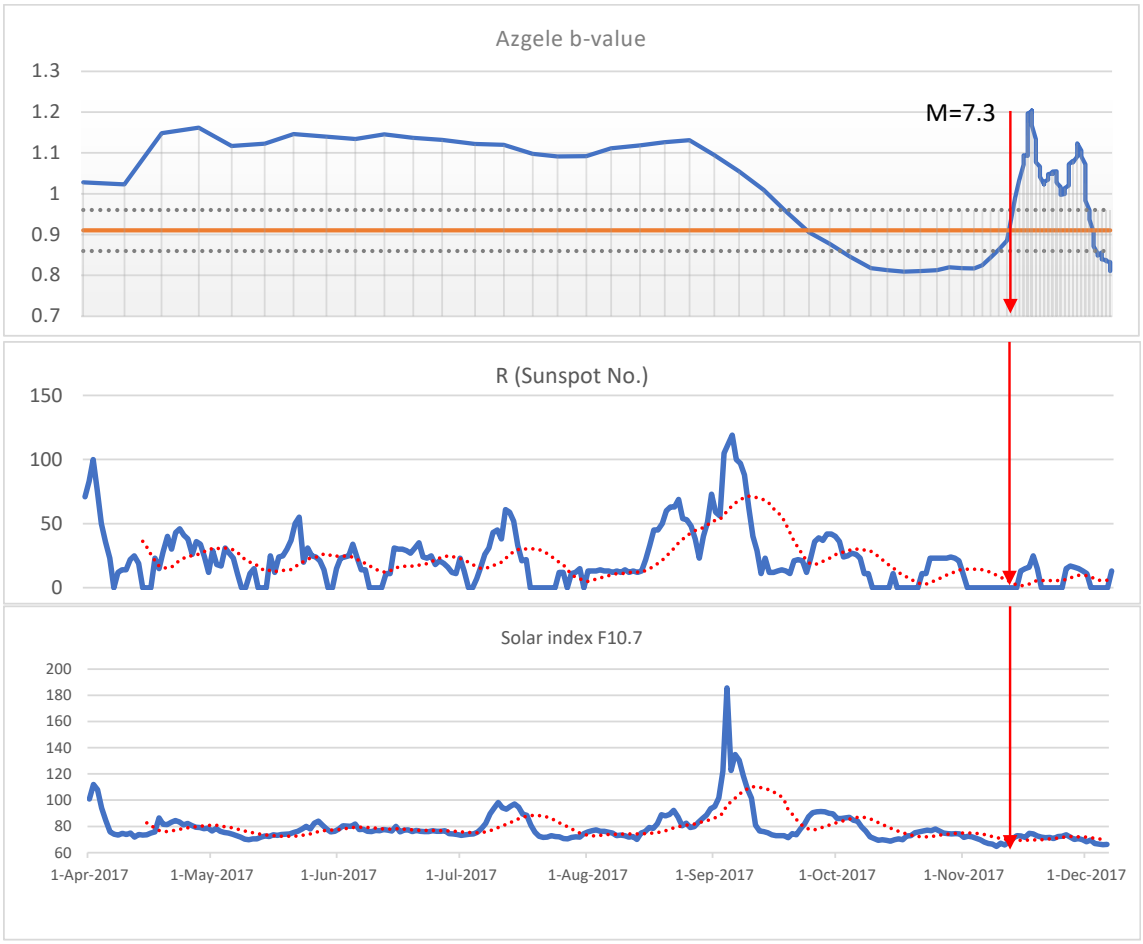


**Figure 11.** The variations of the b-value over time for the Ezgele region events (top), the variations of the sunspot number parameter (middle), and the F10.7 solar radio flux parameter (bottom) with a 1-day resolution. The red dashed lines show the 15-day moving average. The red arrow indicates the day of the largest event.

earthquakes in the New Zealand region occurred with a good correlation coefficient during the solar cycle minima (minimum sunspot number and F10.7 index). However, Han et al. (2004) did the same study for the China and Mongolia regions and came to a different conclusion. Therefore, it seems that to investigate the effect of the solar cycle on seismicity, the seismotectonic conditions must be taken into account. Our research was consistent with Nikouravan's study in this regard. Therefore, to study the magnetic parameters and their effects on seismicity, the position within the solar cycle must first be considered.

After determining the position in terms of the solar cycle, now each of the parameters can be examined at lower resolutions (27 days, 1 day, hourly).

Figures 14 and 15 show the sunspot numbers and F10.7 index, respectively, from March 5, 2017 (30 days before the first seismic event, Sefid Sang) to February 20, 2018 (30 days after the last seismic event, Sumar). In these two figures, it is clear that 4 out of 5 events occurred on days when these two parameters were at their lowest. These findings are consistent with the conclusions of Nikouravan (2012).

Cataldi et al. (2016) in their paper examined the relationship between proton density, interplanetary magnetic field (IMF), and also the Dst index on the occurrence of large earthquakes. They concluded that high-intensity seismic events (M6+) that occur on a global scale always occur after an increase in solar wind proton density. Although the hourly and daily resolutions of proton density in our study do not clearly support such a proposition, the 27-day resolution of this parameter indicates that Cataldi et al. (2016)'s conclusion is also true for our events (Figure 8 and Figure 16). Marchetti et al. (2020) also reached a similar conclusion, which shows that the atmospheric proton density has a high correlation with large seismic events.

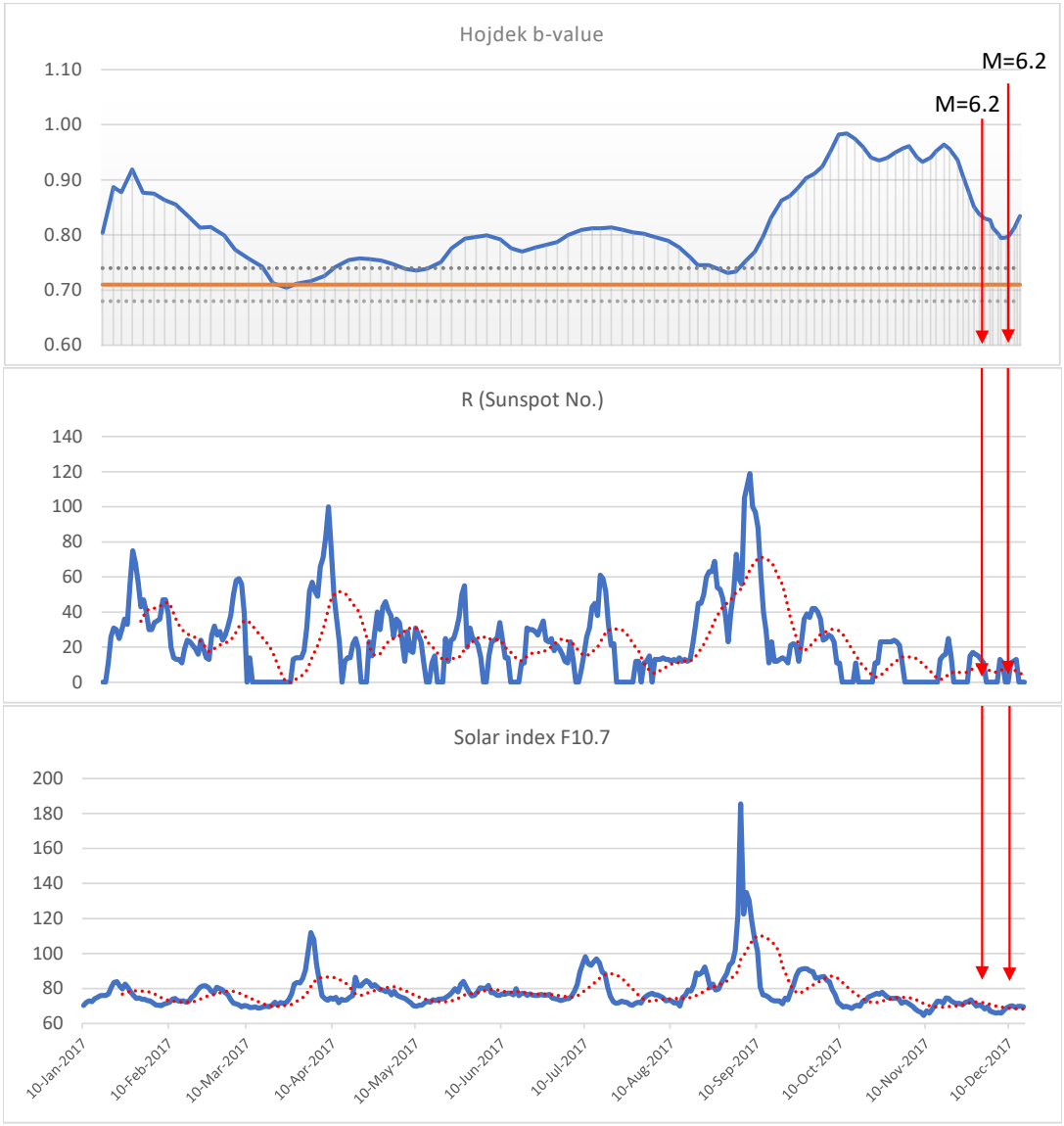


**Figure 12.** The variations of the b-value over time for the Hojdek region events (top), the variations of the sunspot number parameter (middle), and the F10.7 solar radio flux parameter (bottom) with 1-day resolution. The red dashed lines show the 15-day moving average.

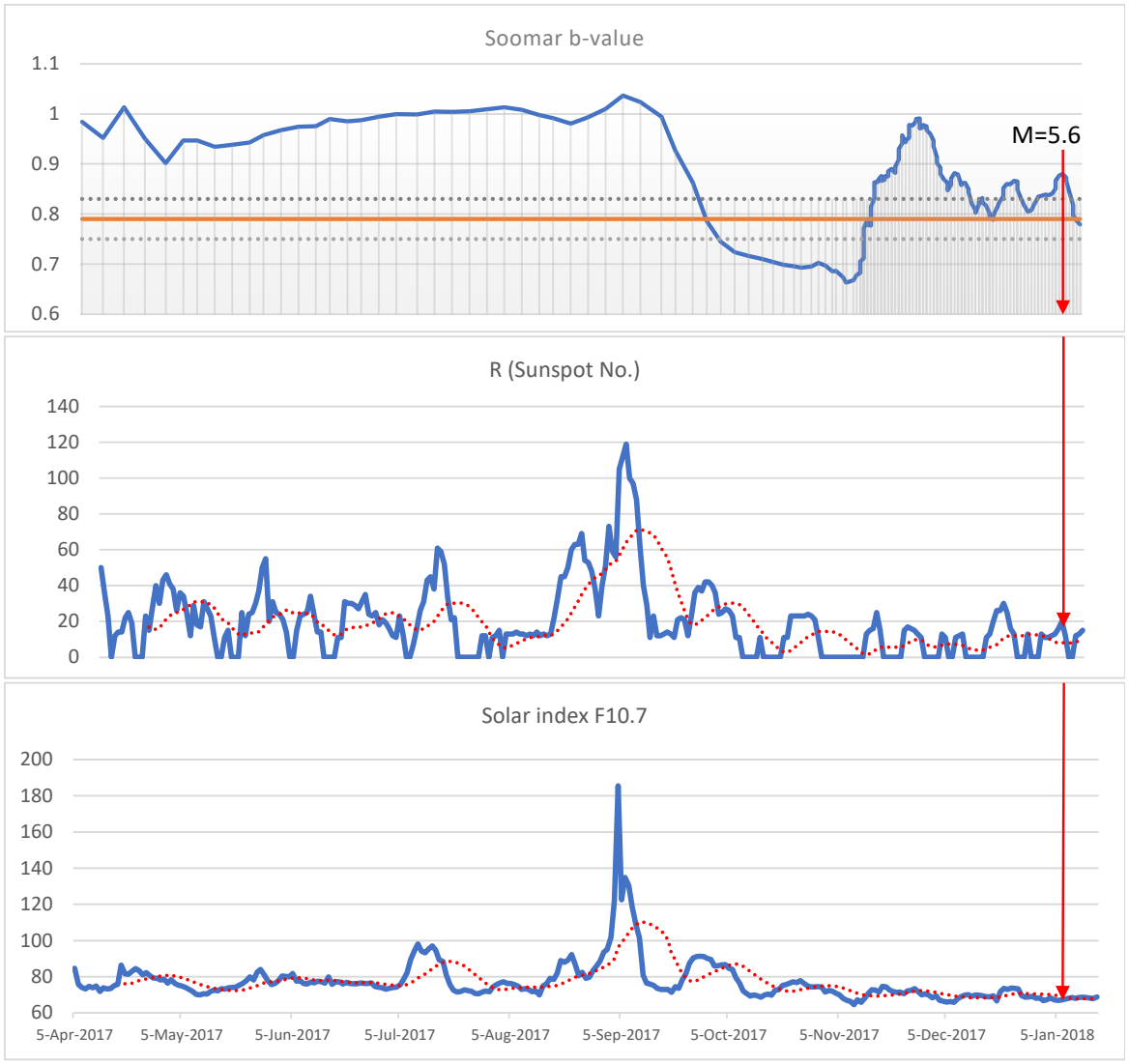


**Figure 13.** The variations of the b-value over time for the Sumar events (top), the variations of the sunspot number parameter (middle), and the F10.7 solar radio flux parameter (bottom) with 1-day resolution. The red dashed lines show the 15-day moving average. The red arrow indicates the day of the largest event.

Regarding the Dst index, they concluded that a large earthquake like the M7 Japan earthquake occurred when this index was experiencing fewer fluctuations and was approaching zero in an increasing path (Figure 18). All 5 regions studied here occurred after a gradual decrease and increase in the 1-hour resolution Dst index (Figure 9C). Also, Fig. 9 with 27-day resolution shows that the main events occurred when the Dst index was close to zero. Figure 17 plots this parameter at 1-day resolution along with the moving average, showing that on the days when the last 4 earthquakes occurred, this parameter was close to zero with little fluctuation.

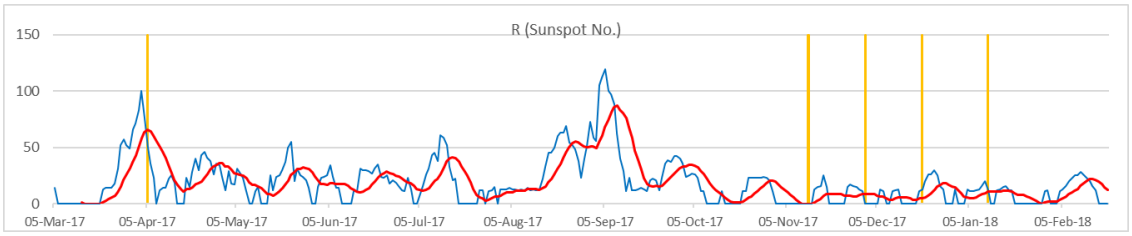


**Figure 14.** Number of sunspots with 1-day resolution from March 5, 2017 (thirty days before the first seismic event, Sefid Sang) to February 20, 2018 (thirty days after the last seismic event of Sumar). The orange vertical lines represent the color of the day of events. The red line is a 10-day moving average.

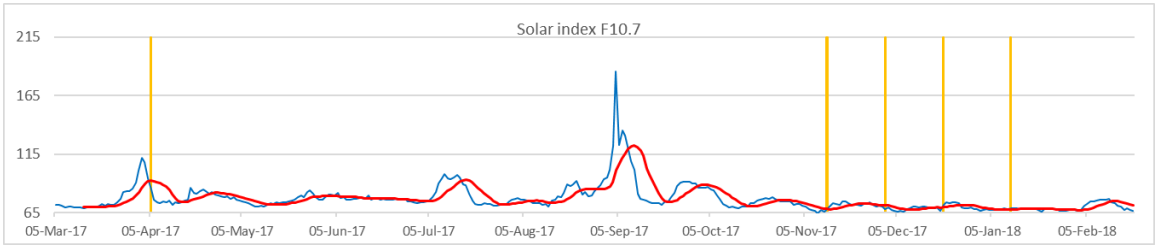


**Figure 15.** 1-day resolution solar F10.7 index from March 5, 2017 (thirty days before the first seismic event, White Rock) to February 20, 2018 (thirty days after the last seismic event of Sumar). The orange vertical lines represent the color of the day of events. The red line is a 10-day moving average.

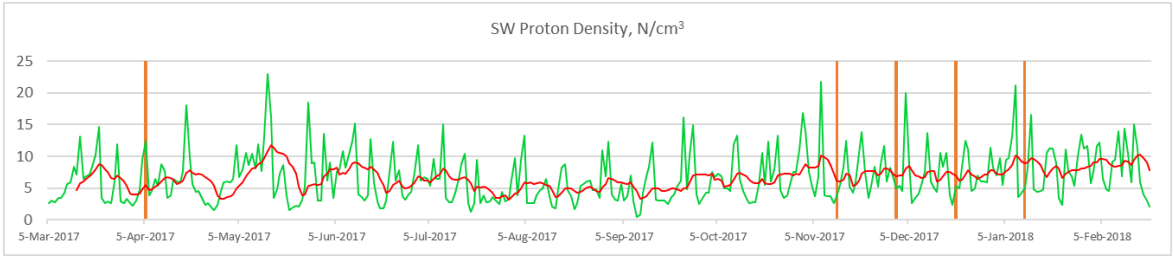


**Figure 16.** Proton density with a 1-day resolution from March 5, 2017 (thirty days before the first seismic event, White Rock) to February 20, 2018 (thirty days after the last seismic event of Sumar). The orange vertical lines represent the color of the day of events. The red line is a 10-day moving average.

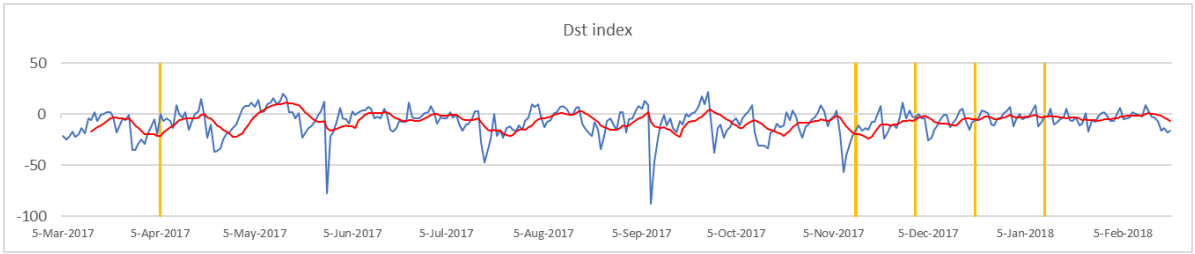


**Figure 17.** DST index with a 1-day resolution from March 5, 2017 (thirty days before the first seismic event, Sefid Sang) to February 20, 2018 (thirty days after the last seismic event of Sumar). The orange vertical lines represent the color of the day of events. The red line is a 10-day moving average.

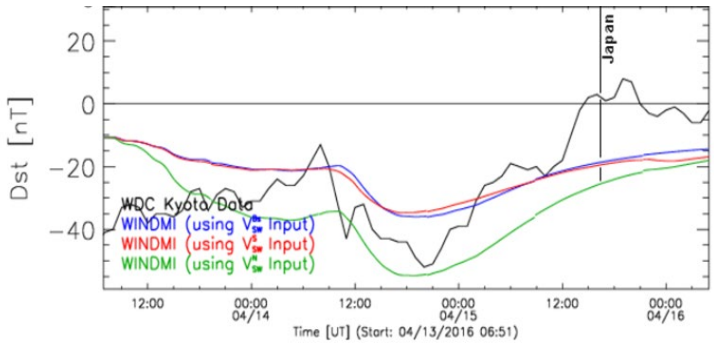


**Figure 18.** Changes in the Dst index for 48 hours before the M7 event in Japan, indicated that the index was approaching zero (Cataldi et al. 2016).

## 4 Conclusion

This study investigated temporal changes in seismicity and magnetic parameters before five earthquakes with magnitudes greater than 5-6 in Iran during 2017-2018, with particular focus on b-value evolution and solar-geomagnetic activity. By combining declustered seismic catalogs from IRSC with multi-resolution solar and geomagnetic indices (sunspot number, F10.7 index, proton density, Dst and Kp), the analysis aimed to explore whether systematic temporal associations exist between crustal seismic processes and external solar-magnetic forcing. However, it should be noted that these findings are based on a relatively small sample size of five mainshocks within a single year, which may limit their broader generalizability and necessitates further validation across diverse tectonic environments to rule out potential sampling biases.

From a seismic perspective, the results show that in four out of five examined regions, the b-value exhibited notable temporal variations in the weeks prior to the mainshock, often characterized by a decrease followed by a partial recovery. Such b-value drops are qualitatively consistent with the idea of increasing differential stress and growing dominance of larger-magnitude events before major failures, as reported in other tectonic settings (Wu et al., 2018). While these patterns are suggestive, their robustness is inherently linked to methodological factors - such as the choice of declustering algorithms (e.g., Reasenberg vs. Gardner-Knopoff) and catalog-specific biases - meaning they should be interpreted as indicative of stress evolution rather than as deterministic precursors (Godano et al., 2014).

Investigation of b-value changes for each region showed that, in four out of the five events, the b-value exhibited a pronounced decrease (typically 20-30%) 15-30 days prior to the mainshock. This pattern aligns with extensive prior research documenting significant spatio-temporal reductions in b-value near future epicenters before large earthquakes [e.g., Gulia et al., 2020; Suyehiro, 1964, 1966; Gibowicz, 1973; Papazachos, 1975; Papadopoulos & Minadakis, 2016; Dascher-Cousineau et al., 2020; Wu et al., 1976]. These decreases are commonly interpreted as reflecting stress concentration and a shift toward larger-event dominance during the nucleation phase, and have proven effective in medium- to long-term seismic hazard monitoring in various tectonic settings. While these temporal alignments are noteworthy, the mismatch between the daily resolution of solar indices and the

15-30-day windows required for stable b-value estimation may reduce sensitivity to shorter-term fluctuations and could potentially obscure more complex sub-monthly interactions.

Regarding magnetic and solar parameters, four of the five mainshocks occurred during intervals when sunspot numbers and the F10.7 index were close to their minimum values within the study period, while the 27-day mean proton density tended to be elevated near the same windows. In addition, Dst and Kp indices showed local anomalies within ±48 hours of several mainshocks, especially for the M7.3 Ezgeleh-Sarpol Zahab event. These findings align qualitatively with earlier reports that large earthquakes may cluster near low solar activity phases or during specific geomagnetic conditions (Nikouravan, 2012; Cataldi et al., 2016; Marchitelli et al., 2020), although other studies have found weak, region-dependent or even contradictory relationships (Han et al., 2004; Novikov et al., 2020). Furthermore, the current study relies on independent visual comparisons rather than integrated physical models; thus, the observed precursors should be viewed as suggestive indicators until formal cross-correlation or stress-transfer modeling can be applied to quantify the proposed coupling.

It should be noted that our analysis avoids integrating seismic and magnetic datasets, as quantifying their interactions (e.g., how geomagnetic fluctuations might modulate seismic stress) would demand significant resources and was outside our scope. Some studies have explored such effects (e.g., Novikov et al., 2020), but we focused on independent examinations to visually highlight relative changes. This revealed clearer precursors in seismic data compared to magnetic ones, though the comparison remains observational. Future work could address these interdependencies with appropriate tools, but we have refrained from affirming or denying them here to maintain an exploratory perspective. Ultimately, as the analysis lacks formal statistical testing (such as Monte Carlo simulations) to compare these results against a null hypothesis, these patterns are presented as a basis for hypothesis generation rather than definitive causal inference.

The combined analysis of seismic and magnetic time series suggests that solar and geomagnetic parameters may, under certain conditions, act as additional indicators of changing stress or susceptibility rather than as primary triggers of earthquakes. In particular, the apparent co-occurrence of b-value decreases with low solar activity and enhanced proton density in four of five cases hints at a possible modulation of fault stability by external electromagnetic processes. However, correlation does not imply causation. Earthquake nucleation is fundamentally governed by lithospheric stress accumulation, fault frictional properties, pore-fluid pressure and crustal heterogeneity, whereas solar and geomagnetic variations - if influential at all - likely play a secondary, triggering or modulating role superimposed on tectonic loading. The small event sample, lack of formal statistical tests, and absence of physically constrained stress-transfer models preclude any causal inference at this stage. Taken together, these methodological constraints confirm the exploratory rather than confirmatory nature of the present work, and should be borne in mind when interpreting the patterns reported above.

Despite these caveats, the study contributes to the growing body of literature exploring multi-parameter approaches to earthquake research. It demonstrates

that, with careful treatment of catalog completeness and magnetic data resolution, joint analysis of seismic and solar-geomagnetic time series can reveal non-trivial temporal structures deserving further investigation. At the current level of evidence, changes in solar parameters and magnetic indices should be regarded as potential statistical indicators of changing seismic likelihood, not as reliable predictive tools. They may complement, but not replace, conventional seismotectonic and probabilistic hazard analyses.

Future work should address the outlined limitations by: (i) extending the analysis to longer time windows and multiple regions with diverse tectonic regimes; (ii) incorporating formal statistical methods (e.g., Monte Carlo simulations, cross-correlation and superposed epoch analysis, forecast skill scores) to test whether the observed temporal coincidences exceed random expectations; (iii) systematically comparing different declustering algorithms and b-value estimation techniques to assess methodological robustness; and (iv) coupling observational analyses with physically based models of solar wind-magnetosphere-ionosphere-lithosphere coupling to quantify plausible stress perturbations at seismogenic zone. Future studies could also undertake a detailed quantification of IRSC error propagation on b-value estimates and other seismic parameters, potentially as an independent project to enhance catalog reliability. Only through such multi-disciplinary and prospective studies can the scientific community determine whether solar and geomagnetic parameters genuinely carry usable information about the timing or probability of future earthquakes, or whether the apparent correlations observed so far mainly reflect statistical fluctuations in complex natural systems.

## References


Allan, R. S., & Mason, S. G. (1962). Particle behaviour in shear and electric fields I. Deformation and burst of fluid drops. Proceedings of the Royal Society of London. Series A. Mathematical and Physical Sciences, 267(1328), 45-61.

Amitrano, D. (2003). Brittle-ductile transition and associated seismicity: Experimental and numerical studies and relationship with the b value. Journal of Geophysical Research: Solid Earth, 108(B1).

Calandra, S., & Teti, D. (2024). Correlation Study: Triggering and Magnitude of Earthquakes in Italy (≥ M4. 3) in Relation to the Positions and Gravitational Forces of the Sun, Moon, and Planets Relative to Earth. *New Concepts in Global Tectonics Journal*, *12*(1).

Cataldi, G., Cataldi, D., & Straser, V. (2016). Solar activity correlated to the M7. 0 Japan earthquake occurred on April 15, 2016. New Concepts in Global Tectonics Journal, 4(2), 202-208.

Cauzzi, C., Behr, Y., Le Guenan, T., Douglas, J., Auclair, S., Woessner, J., ... & Wiemer, S. (2016). Earthquake early warning and operational earthquake forecasting as real-time hazard information to mitigate seismic risk at nuclear facilities. Bulletin of Earthquake Engineering, 14, 2495-2512.

Chung, D. H., & Bernreuter, D. L. (1980). Seismic Safety Margins Research Program. Regional relationships among earthquake magnitude scales (No. NUREG/CR-1457; UCRL-52745). Lawrence Livermore National Lab., CA (USA).

Dascher-Cousineau, K.; Lay, T.; Brodsky, E.E. Two foreshock sequences post gulia and wiemer (2019). Seismol. Res. Lett. 2020, 91, 2843-2850.

de Arcangelis, L., Lippiello, E., Godano, C., & Nicodemi, M. (2008). Statistical properties and universality in earthquake and solar flare occurrence. The European Physical Journal B, 64, 551-555.

Galper, A. M., S. V. Koldashov, and S. A. Voronov. "High energy particle flux variations as earthquake predictors." Advances in Space Research 15.11 (1995): 131-134.

Gardner, J. K., & Knopoff, L. (1974). Is the sequence of earthquakes in Southern California, with aftershocks removed,

Poissonian?. Bulletin of the seismological society of America, 64(5), 1363-1367.

Gibowicz, S.J. Variation of the frequency-magnitude relation during earthquake sequences in new zealand. Bull. Seismol. Soc. Am. 1973, 63, 517-528.

Godano, C., Lippiello, E., & de Arcangelis, L. (2014). Variability of the b value in the Gutenberg-Richter distribution. Geophysical Journal International, 199(3), 1765-1771.

Gulia, L.; Wiemer, S.; Vannucci, G. Pseudo-prospective evaluation of the foreshock traffic-light system in Ridgecrest and implications for aftershock hazard assessment. Seismol. Res. Lett. 2020, 91, 2828-2842.

Gutenberg, B., & Richter, C. F. (1944). Frequency of earthquakes in California. Bulletin of the Seismological Society of America, 34(4), 185-188.

Han, Y., Guo, Z., Wu, J., & Ma, L. (2004). Possible triggering of solar activity to big earthquakes (Ms≥ 8) in faults with near west-east strike in China. Science in China Series G: Physics and Astronomy, 47, 173-181.

Jackson, D. D., & Kagan, Y. Y. (1999). Testable earthquake forecasts for 1999. Seismological Research Letters, 70(4), 393-403.

Keilis-Borok, V., & Soloviev, A. A. (Eds.). (2002). Nonlinear dynamics of the lithosphere and earthquake prediction. Springer Science & Business Media.

Loewe, C. A., & Prölss, G. W. (1997). Classification and mean behavior of magnetic storms. Journal of Geophysical Research: Space Physics, 102(A7), 14209-14213.

Marchitelli, V., Harabaglia, P., Troise, C., & De Natale, G. (2020). On the correlation between solar activity and large earthquakes worldwide. Scientific reports, 10(1), 11495.

Márquez-Ramírez, V. H., Nava, F. A., & Zúñiga, F. R. (2015). Correcting the Gutenberg-Richter b-value for effects of rounding and noise. Earthquake Science, 28, 129-134.

Marzocchi, W., Lombardi, A. M., & Casarotti, E. (2014). The establishment of an operational earthquake forecasting system in Italy. Seismological Research Letters, 85(5), 961-969.

Menvielle, M., & Berthelier, A. (1991). The K-derived planetary indices: description and availability. Reviews of Geophysics, 29(3), 415-432.

Moradi, A., Dezvareh, M., & Rahmati, M. (2016). Review of the statistics of earthquakes in Iran in 2016. In M. Naqvi, H. Rahimi, & A. Moradi (Chairs), 18th Iran Geophysics Conference, Tehran.

Naserieh, S., Karkooti, E., Dezvareh, M., et al. (2019). Analysis of artifacts and systematic errors of the Iranian Seismological Center's earthquake catalog. Journal of Seismology, 23, 665-682. https://doi.org/10.1007/s10950-019-09828-z

Nikouravan, B. (2012). Do Solar Activities Cause Local Earthquakes?(New Zealand): Earthquake. International Journal of Fundamental Physical Sciences, 2(2), 17-20.

Novikov, V., Ruzhin, Y., Sorokin, V., & Yaschenko, A. (2020). Space weather and earthquakes: possible triggering of seismic activity by strong solar flares. Annals of Geophysics, 63(5), PA554-PA554.

Omori, F. (1894). On the aftershocks of earthquakes. Journal of the College of Science, Imperial University of Tokyo, 7, 111-200.

Papadopoulos, G.A.; Minadakis, G. Foreshock patterns preceding great earthquakes in the subduction zone of chile. Pure Appl. Geophys. 2016, 173, 3247-3271.

Papazachos, B.C. Foreshocks and earthquake prediction. Tectonophysics 1975, 28, 213-226.

Poudyal Lohani, Dibyashree & Nordin, Norhaiza & Roslan, Siti Nur Aliaa. (2025). Comparative Declustering Approaches for Seismic Data: Insights from Gardner-Knopoff, Gruenthal, Reasenberg, and Uhrhammer in the Kathmandu Valley. Annals of Geophysics. 68. NH215. 10.4401/ag-9178.

Reasenberg, P. (1985). Second-order moment of central California seismicity, 1969-1982. Journal of Geophysical Research: Solid Earth, 90(B7), 5479-5495.

Saltiel, S., Boyle, K., & Majer, E. (2011). Challenges in determining b value in the Northwest Geysers (No. LBNL-4594E). Lawrence Berkeley National Lab.(LBNL), Berkeley, CA (United States).

Senatorski, P. (2020). Gutenberg-Richter'sb value and earthquake asperity models. Pure and applied Geophysics, 177(5), 1891-1905.

Shi, Y., & Bolt, B. A. (1982). The standard error of the magnitude-frequency b value. Bulletin of the Seismological Society of America, 72(5), 1677-1687.

Simpson, J. F. (1967). Solar activity as a triggering mechanism for earthquakes. Earth

and Planetary Science Letters, 3, 417-425.
Stein, S., & Wysession, M. (2009). An introduction to seismology, earthquakes, and earth structure. John Wiley & Sons.
Suyehiro, S. Difference between aftershocks and foreshocks in the relationship of magnitude to frequency of occurrence for the great chilean earthquake of 1960. Bull. Seismol. Soc. Am. 1966, 56, 185-200.
Suyehiro, S.; Asada, T.; Ohtake, M. Foreshocks and aftershocks accompanying a perceptible earthquake in central japan: On the peculiar nature of foreshocks. Pap. Meteorol. Geophys. 1964, 15, 71-88.
Tavares, M., & Azevedo, A. (2011). Influences of solar cycles on earthquakes. Natural Science, 3(06), 436.
Teng, G., & Baker, J. W. (2019). Seismicity declustering and hazard analysis of the Oklahoma-Kansas region. Bulletin of the Seismological Society of America, 109(6), 2356-2366.
Urata, N., Duma, G., & Freund, F. (2018). Geomagnetic Kp index and earthquakes. Open Journal of Earthquake Research, 7(1), 39-52.
Venegas-Aravena, P., & Cordaro, E. G. (2023). Analytical relation between b-value and electromagnetic signals in pre-macroscopic failure of rocks: insights into the microdynamics' physics prior to earthquakes. *Geosciences*, *13*(6), 169.
Wesseloo, J. (2014). Evaluation of the spatial variation of b-value. Journal of the Southern African Institute of Mining and Metallurgy, 114(10), 823-828.
Wu, K.T.; Yue, M.S.; Wu, H.Y.; Cao, X.L.; Chen, H.; Huang, W.Q.; Tian, K.Y.; Lu, S.D. Certain characteristics of Haicheng earthquake sequence. Acta Geophys. Sin. 1976, 19, 95-109, (In Chinese with English Abstract).
Wu, Y. M., Chen, S. K., Huang, T. C., Huang, H. H., Chao, W. A., & Koulakov, I. (2018). Relationship between earthquake b-values and crustal stresses in a young orogenic belt. Geophysical Research Letters, 45(4), 1832-1837.